Low-Temperature Specific Heat of $La_{1-x}Sr_xMnO_{3+\delta}$

B. F. Woodfield,* M. L. Wilson,† and J. M. Byers
Naval Research Laboratory, Washington, D.C. 20375
(Received 8 November 1996)

The specific heat of the perovskite manganite $La_{1-x}Sr_xMnO_{3+\delta}$ was measured in the doping regime $x = 0.0$ to 0.3 where at low temperatures the material changes from a layered antiferromagnetic insulator to a ferromagnetic metal. A term in the specific heat, $C \propto T^2$, is found in $LaMnO_3$ that is attributable to spin excitations in a layered antiferromagnet. Ferromagnetic samples have the expected specific heat term $C \propto T^{3/2}$ due to ferromagnetic spin waves. The exchange coupling (J), electronic linear term (γ), Debye temperature (θ_D), and the local field at the Mn site (H_{hyp}) are extracted from the specific heat as functions of Sr doping. [S0031-9007(97)02950-5]

PACS numbers: 75.40.Cx, 71.30.+h, 72.80.Ga, 75.30.Ds

The perovskite manganites exhibit many interesting properties associated with the connection between charge transport and magnetic structure [1]. Most work focuses on the magnetoresistive properties that are most pronounced in the $x = 0.3$ compounds of $[RE]_{1-x}II_xMnO_{3+\delta}$ where RE is a lanthanide and II is a divalent cation [2]. The goal of this study is different in that the metal-insulator transition as a function of temperature and applied field will be ignored and, instead, the nature of the transition as a function of x at low temperatures was studied.

To examine how the low-temperature metallic phase evolves with doping from the parent compound, in this case $LaMnO_3$ doped with Sr, high-precision specific-heat measurements were performed on samples screened by resistivity and dc magnetization measurements. The specific heat has been previously measured for a range of dopings x but only for $T \geq 50$ K in $La_{1-x}Ca_xMnO_3$ [3]. The specific heat of the doped manganites have been measured for fixed x where the divalent cation has been varied (Ca, Sr, and Ba) [4] and for samples of Ca-doped $x = 0.2$ [5] and $x = 0.33$ [6]. With doping, $La_{1-x}Sr_xMnO_{3+\delta}$ demonstrates marked changes in both its low-energy magnetic and electronic excitations as well as the behavior of the lattice. By fitting the specific heat data at low temperatures the evolution of the magnetic-exchange coupling (J), electronic linear term (γ), Debye temperature (θ_D), and local magnetic field at the Mn site (H_{hyp}) can be extracted as functions of doping.

Samples for this study were prepared using a standard grind and fire method. Pure powders of La_2O_3, SrO, and MnO were stoichiometrically mixed, pressed into a pellet, and fired in air at 1300 °C for 20 hours. The pellets were then air quenched, reground, and refired under identical conditions three additional times. The final pellets were 12.5 or 10 mm in diameter having masses of 2–3 g with nominal Sr concentrations of 0.00, 0.10, 0.20, and 0.30. All measurements for each Sr concentration were performed on samples from the same firing run.

Two screening tests were performed on each sample: electrical resistivity and dc magnetization. For $x = 0.1$ the sample has a small local maximum in the resistivity at 235 K with an overall resistivity that increases exponentially with decreasing temperature (insulating). For $x = 0.2$ and 0.3, the resistivity passes through a peak at a temperature T_p (320 and 370 K for 0.2 and 0.3, respectively) with activated behavior above and metallic conduction below T_p. The Curie temperatures T_C extracted from magnetization data were 145, 250, and 310 K for the 0.0, 0.1, and 0.2 samples, respectively. Compared to magnetization measurements on $La_{1-x}Sr_xMnO_{3+\delta}$ single crystals [7], our $x = 0.1$ sample appears to have excess oxygen of $\delta \approx 0.02$ to yield an elevated Curie temperature. We were unable to measure T_C for the 0.3 sample due to the large value.

Specific-heat measurements were performed from 0.5 to 200 K in zero magnetic field. A semiadiabatic technique [8] was used to measure the specific heat from 0.5 to 20 K having a precision of $\pm 0.1\%$ and an accuracy typically better than 0.5% as compared to accepted values [9]. Above 20 K, an isothermal technique was used [10] having a precision of $\pm 0.1\%$ and an accuracy better than 0.25% below 100 K but increasing to 1.5% at 200 K [11]. Details on the specific-heat apparatus and the results on copper are described elsewhere [12].

The results of the specific-heat measurements below 10 K are shown in Fig. 1 plotted as C/T versus T with T on a log scale in order to expand the low-temperature region. The first obvious feature is a low-temperature upturn present in all samples indicative of a Mn-hyperfine contribution to the specific heat (C_{hyp}). This term is caused by the large local magnetic field at the Mn nucleus (H_{hyp}) due to electrons in unfilled shells. C_{hyp} can be adequately represented by A_{-2}/T^2 and the coefficient converted to a local field (H_{hyp}) at the Mn nucleus [13]. When the data are plotted as C/T versus T with T on a linear scale (see inset to Fig. 1), the $x = 0.0$ data show a conspicuous linear dependence above 1.5 K strongly suggesting a T^2 temperature dependence to the specific heat; however, for the $x = 0.1$, 0.2, and 0.3 data, no such T^2 dependence seems obvious. To isolate this term, fits

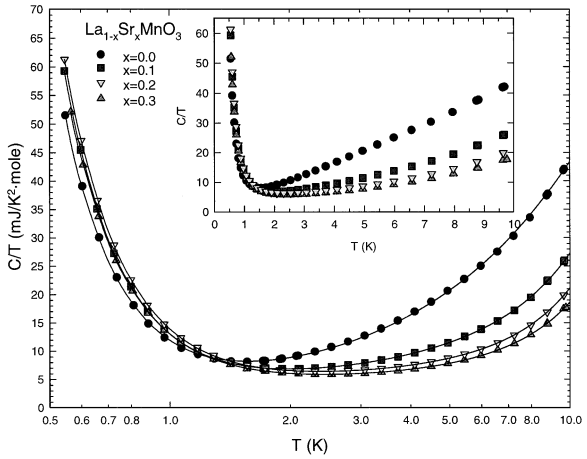

FIG. 1. The low-temperature specific heat for $x = 0.0$, 0.1, 0.2, and 0.3 from $T = 0.5$ to 10 K plotted on a linear-log scale as C/T vs T. The lines are the best fits to the data as listed in Table I. The inset shows the same data on a linear-linear scale.

were performed on each set of data to the equation

$$C = C_{\mathrm{mag}} + C_{\mathrm{elec}} + C_{\mathrm{lat}} + C_{\mathrm{hyp}}\,, \tag{1}$$

where C_{mag} is the spin-wave contribution to the specific heat varying as $B_{3/2}T^{3/2}$ or B_2T^2, C_{elec} is the electronic contribution γT, C_{lat} is the lattice contribution $B_3T^3 + B_5T^5$, and C_{hyp} is described above.

Shown in Table I are the results and %rms deviations of the most relevant fits performed on the data. The first fit for each sample is considered to be the best fit for that sample. The other fits demonstrate the effects of adding or removing terms in Eq. (1) with their resultant change in %rms deviation. The use of the B_5T^5 term in the lattice contribution is required to adequately fit each data set below 10 K. Narrowing the fitting region from either the low- or high-temperature side does not significantly change the parameters except to eliminate the need for the B_5T^5 term. The lines through each data set in Fig. 1 were generated using the best fits in Table I.

From the fitting results, it is clear that for the $x = 0.0$ sample there is a T^2 contribution to the specific heat which disappears in the Sr-doped samples. $LaMnO_3$ is a type-*A* antiferromagnet (ferromagnetic layers antiferromagnetically coupled) [14]. Inelastic neutron scattering on other layered antiferromagnets (e.g., NiO and MnO) find both linear and quadratic dispersion relations depending on the orientation being probed within the magnetic Brillouin zone [15]. Therefore, we propose the following dispersion relation for the long-wavelength spin excitations:

$$\omega = D_\rho k_\rho^2 + D_z|k_z|\,, \tag{2}$$

where $k_\rho = \sqrt{k_x^2 + k_y^2}$ and D_ρ and D_z are the spin-wave stiffness coefficients for the planar ferromagnetic and linear antiferromagnetic excitations, respectively. This dispersion relation yields the low-temperature magnetic contribution to the specific heat per unit volume,

$$C_{\mathrm{mag}} = \frac{3k_B}{4\pi^3 D_\rho D_z}\left[\int_0^\infty dx \int_0^\infty dy\, \frac{x + y}{e^{x+y} - 1}\right](k_BT)^2, \tag{3}$$

offering a plausible candidate for the observed T^2 contribution in the $x = 0.0$ sample [16]. From the experimental value of B_2 and Eq. (3) the spin-wave stiffness product $D_\rho D_z = 55\ (\mathrm{meV})^2\,\text{Å}^3$. The presence of the $T^{3/2}$ term and the disappearance of the T^2 in the $x = 0.1$, 0.2, and 0.3 samples indicates that type-*A* antiferromagnetic order has been replaced by ferromagnetic order.

The other contribution to C of interest is C_{elec}. From Table I, it is clear that for the $x = 0.0$ and 0.1 samples no linear term is necessary in the fitting expression confirming the resistivity measurements that these samples are insulators. For the $x = 0.2$ and 0.3 samples, the linear terms are necessary and are roughly the same at 3.3 $\mathrm{mJ/K^2}$ mole. A linear term for $La_{0.7}Sr_{0.3}MnO_3$ has been reported elsewhere [4] and is significantly larger at 6.0 $\mathrm{mJ/K^2}$ mole; however, their data extend to only 2 K and C_{hyp} and C_{mag} were not included. Fitting the $x = 0.3$

TABLE I. Summary of fitting results to the data in Fig. 1. The definition of the coefficients are given in the text. The units are $\mathrm{mJ/mole\,K^{n+1}}$ where n is the subscript of the coefficient. The asterisk denotes the best fit.

x	A_{-2}	γ	$B_{3/2}$	B_2	$B_3 \times 10^2$	$B_5 \times 10^4$	% rms
0.0*	8.0340	···	···	3.8003	7.0610	−1.6792	1.00
0.0	6.8872	4.9406	···	···	72.129	−35.217	6.22
0.0	7.5352	···	4.1606	···	50.515	−21.000	3.58
0.1*	9.2035	···	3.7024	···	11.693	3.9655	0.51
0.1	9.1534	0.292 35	3.4727	···	12.722	3.3373	0.47
0.1	8.4419	4.6551	···	···	28.719	−6.6046	2.89
0.2*	9.2977	3.3386	1.1802	···	9.6989	4.4033	0.36
0.2	9.9110	···	3.7516	···	−1.3083	10.952	2.40
0.2	9.0338	4.8505	···	···	14.894	1.2557	1.14
0.3*	8.6913	3.2873	0.95672	···	8.3828	3.9763	0.41
0.3	8.4647	4.5291	···	···	12.493	1.5227	1.07
0.3	9.3234	···	3.4492	···	−1.9837	10.038	2.62

data reported here under similar conditions yields a linear term of approximately 6 mJ/K^2 mole.

The behavior of γ suggests a metal-insulator transition between $x = 0.1$ and 0.2 with the surprise that upon further doping to $x = 0.3$ there is no increase in γ. The linear term in the specific heat of a metal can be related to the density of states at the Fermi surface $N(E_F)$: $\gamma = \pi^2 k_B^2 N(E_F)/3$. Using $\gamma = 3.3$ mJ/K^2 mole yields a $N(E_F) = 2.4 \times 10^{22}/\text{eV cm}^3$ which compares favorably to the value $N(E_F) = 1.4 \times 10^{22}/\text{eV cm}^3$ determined from band-structure calculations for $La_{0.67}Ca_{0.33}MnO_3$ [17]. This result suggests that the mass enhancement due to interactions is not of overwhelming importance in the metallic state of $La_{1-x}Sr_xMnO_3$.

Photoemission spectroscopy purports that the Fermi energy lies in the conduction band with increasing density of states towards higher energy [18]. If true, the Fermi surface is electron-like and samples should be considered as electron-doped $SrMnO_3$ with a carrier concentration n of $(1 - x)$ per unit cell (to yield $n = 1.2 \times 10^{22}$ cm^{-3} for $x = 0.3$). Using the free-electron gas relation $N(E_F) = 3n/2E_F$ yields an upper bound on the Fermi energy of 700 meV. The available phase space for electron-electron scattering is proportional to $(k_B T/E_F)^2$ so that a small Fermi energy enhances this scattering channel over others but the interaction strength is *not* necessarily stronger than systems with large Fermi energies [19]. $E_F = 700$ meV is a low value compared to common metals and implies that electron-electron scattering may dominate over other scattering mechanisms. The resistivity of the $x = 0.2$ and 0.3 samples shows $\rho = \rho_0 + AT^2$ behavior for $T \leq 200$ K as previously reported for $La_{1-x}Sr_xMnO_3$ [7]. This indicates a strong component of electron-electron scattering via phonons or spin excitations as might be expected from a magnetic material with a low-carrier density (small Fermi energy).

Shown in Fig. 2 are the relevant fitting parameters in Table I converted to J, γ, θ_D, and H_{hyp} plotted versus x. For the dopings $x = 0.1$, 0.2, and 0.3 the magnetic-exchange coupling J is determined using the standard formula for spin excitations in a simple cubic ferromagnet [20]. The increase in J tracks the increase of the Curie temperature T_C. For the $x = 0.2$ sample ($T_C = 320$ K) the $J = 1.9$ meV. This value can be compared to $J \approx 1$ meV found in $La_{0.8}Ca_{0.2}MnO_3$ with the majority of the difference attributable to the lower Curie temperature ($T_C = 208$ K for $x = 0.2$) [5]. One should also note that J in this Letter is extracted from the low-temperature specific heat, whereas J in Ref. [5] was taken from the change in entropy as determined from the anomaly in the specific heat near the Curie temperature.

For the $x = 0.3$ sample ($T_C \approx 375$ K) the $J = 2.3$ meV which compares favorably to $J = 2.4$ meV in $La_{0.7}Pb_{0.3}MnO_3$ ($T_C = 355$ K) determined via neutron scattering [21]. The spin-wave stiffness coefficient corresponding to $J = 2.3$ meV is $D = 130$ meV Å^2 using the relation $D = 2JSa^2$ with the lattice constant $a = 3.9$ Å and $S = (4 - x)/2$ for $x = 0.3$. This value is in rough agreement with the more direct measurements via inelastic neutron scattering of $D = 188$ meV Å^2 measured at 27 K in $La_{0.7}Sr_{0.3}MnO_3$ [22] and $D = 170$ meV Å^2 at zero temperature in $La_{0.67}Ca_{0.33}MnO_3$ [23]. No need was found for a spin-wave energy gap in the fitting results in Table I for any sample even to the lowest temperatures ($T \geq 0.5$ K) consistent with a soft magnetic material (in agreement with ferromagnetic resonance studies [24]).

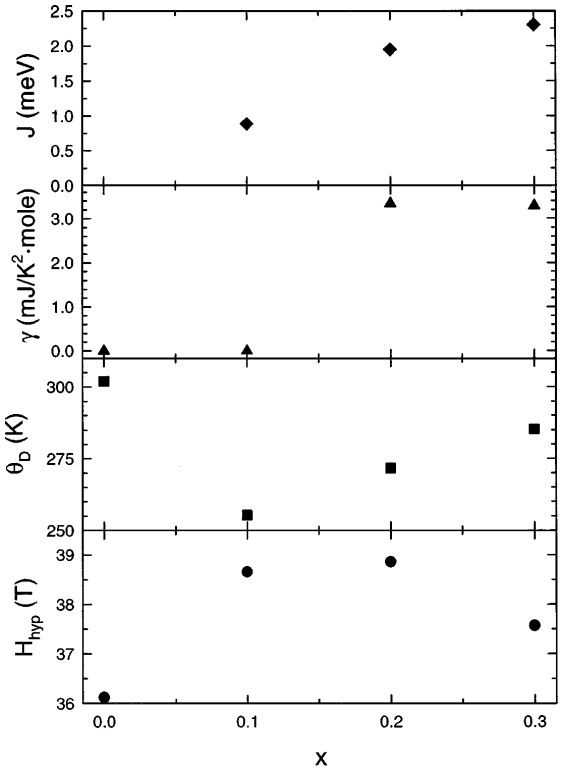

FIG. 2. Plots of the parameters J, γ, θ_D, and H_{hyp} versus doping x as extracted from fitting the data in Fig. 1. The $x = 0.0$ sample is not included in the plot of J since the coupling is not ferromagnetic.

With Sr doping the lattice softens as indicated by the decreasing θ_D in Fig. 2. After going through a minimum near the metal-insulator transition ($x \simeq 0.2$), θ_D increases with the Sr concentration. The softening of the lattice seen here in the specific heat between $x = 0.1$ and 0.2 seems closely related to the magnetic field-induced structural distortions observed in $La_{0.825}Sr_{0.175}MnO_3$ [25]. The magnitude of θ_D reported here is significantly lower than that reported for $La_{0.8}Ca_{0.2}MnO_3$ where $\theta_D = 528$ K, but, again, this value was extracted from data at higher temperatures ($T \geq 100$ K) fit directly to the Debye function [5].

The local magnetic field at the Mn sites can be determined from the nuclear Schottky anomaly for two reasons. The first is that the on-site moment of the electrons is large due to the Hund's rule alignment of spins. This pushes the nuclear Schottky anomaly up to attainable temperatures. The second reason is the useful coincidence that the most prevalent isotope of oxygen (^{16}O with a 99.96%

abundance) has *no* nuclear moment [26]. Although the $e_g - \sigma^*$ conduction band is composed of hybridized Mn $3d$ (e_g) and O $2p$ (σ^*) orbitals, the nuclear Schottky anomaly will only respond to changes on the Mn sites. This provides a means for determining where the doped carriers are residing.

Initially, $H_{\rm hyp}$ increases as the Sr doping x increases. Since Sr introduces holes into the $e_g - \sigma^*$ band of $LaMnO_3$, an increasing $H_{\rm hyp}$ means that the holes must be going to the oxygen sites with electrons being pushed onto the Mn sites. Holes on the oxygen sites mean that the magnetic moment is *not* solely on the Mn sites. This trend continues through the metal-insulator transition to $x = 0.2$. For the $x = 0.3$ sample $H_{\rm hyp}$ decreases implying that holes are finally doped onto Mn sites. These properties identify $LaMnO_3$ as having significant charge-transfer insulating character [27]. These results can be compared to photoemission spectroscopy (PES) on $La_{1-x}Sr_xMnO_{3+\delta}$ where the ground state was found to have a very mixed character of oxygen p and Mn d orbitals [18]. The change of the ground state character measured in PES with doping is consistent with the doped holes going to the oxygen sites as indicated in our measurements.

In conclusion, the low-temperature specific heat of $La_{1-x}Sr_xMnO_{3+\delta}$ reveals that the $x = 0.3$ metallic compound is a low-carrier density metal with conventional ferromagnetic spin waves. The extracted magnetic-exchange coupling (J) and spin-wave stiffness coefficient (D) are in rough agreement with inelastic neutron scattering results. The Debye temperature is found to be lower than previously measured for the perovskite manganites and can vary by 20% with doping of holes that preferentially reside on the oxygen sites.

The authors would like to acknowledge support of this research from National Research Council postdoctoral fellowships. B. W. thanks R. Soulen for considerable experimental assistance.

*Present address: Southern Virginia College, Buena Vista, VA 24416.

†Present address: Department of Physics and Astronomy, Clemson University, Clemson, SC 29634.

[1] G. H. Jonker and J. H. van Santen, Physica (Utrecht) **16**, 337 (1950).

[2] S. Jin, T. H. Tiefel, M. McCormack, R. A. Fastnacht, R. Ramesh, and L. H. Chen, Science **264**, 413 (1994).

[3] A. P. Ramirez, P. Schiffer, S-W. Cheong, C. H. Chen, W. Bao, T. T. M. Palstra, P. L. Gammel, D. J. Bishop, and B. Zegarski, Phys. Rev. Lett. **76**, 3188 (1996).

[4] J. M. D. Coey, M. Viret, L. Ranno, and K. Ounadjela, Phys. Rev. Lett. **75**, 3910 (1995).

[5] J. Tanaka and T. Mitsuhashi, J. Phys. Soc. Jpn. **53**, 24 (1984).

[6] S. N. Bai *et al.*, Chin. J. Phys. **34**, 798 (1996).

[7] A. Urushibara, Y. Moritomo, T. Arima, A. Asamitsu, G. Kido, and Y. Tokura, Phys. Rev. B **51**, 14 103 (1995).

[8] N. E. Phillips *et al.* (to be published).

[9] D. W. Osborne, H. F. Florow, and F. Schreiner, Rev. Sci. Instrum. **38**, 159 (1967).

[10] W. F. Giauque (unpublished).

[11] D. L. Martin, Rev. Sci. Instrum. **58**, 639 (1987).

[12] B. F. Woodfield and R. A. Soulen, Jr. (to be published).

[13] H. Kopfermann, *Nuclear Moments* (Academic Press, New York, 1958).

[14] E. O. Wollan and W. C. Koehler, Phys. Rev. **100**, 545 (1955); Q. Huang, A. Santoro, J. W. Lynn, R. W. Erwin, J. A. Borchers, J. L. Peng, and R. L. Greene (to be published).

[15] M. T. Hutchings and E. J. Samuelsen, Phys. Rev. B **6**, 3447 (1972) (NiO); J. Pepy, J. Phys. Chem. Solids **35**, 433 (1974) (MnO); M. Kohgi, Y. Ishikawa, I. Harada, and K. Motizuki, J. Phys. Soc. Jpn. **36**, 112 (1974) (MnO). These compounds have spin-wave energy gaps and, thus, do not exhibit T^2 dependence in the specific heat [e.g., H. W. White, J. Chem. Phys. **61**, 4907 (1974)].

[16] The prefactor to the integral in Eq. (3) is derived for a magnetic Brillouin zone of extent $\pi/2a$ in the k_z direction because of antiferromagnetic ordering. The integral has a numerical value of 2.40 to yield $C_{\rm mag} = 0.058 k_B (k_B T)^2 / D_\rho D_z$.

[17] W. E. Pickett and D. J. Singh, Phys. Rev. B **53**, 1146 (1996).

[18] A. Chainani, M. Mathew, and D. D. Sarma, Phys. Rev. B **47**, 15 397 (1993); T. Saitoh, A. E. Bocquet, T. Mizokawa, H. Namatame, A. Fujimori, M. Abbate, Y. Takeda, and M. Takano, Phys. Rev. B **51**, 13 942 (1995); J.-H. Park, C. T. Chen, S-W. Cheong, W. Bao, G. Meigs, V. Chakarian, and Y. U. Idzerda, Phys. Rev. Lett. **76**, 4215 (1996).

[19] N. W. Ashcroft and N. D. Mermin, *Solid State Physics* (W.B. Saunders Co., New York, 1976), pp. 346ff.

[20] C. Kittel, *Quantum Theory of Solids* (John Wiley and Sons, Inc., New York, 1987), p. 55. The specific heat per unit volume for ferromagnetic spin waves is $C_{\rm mag} = 0.113 k_B (k_B T/D)^{3/2}$ for the dispersion relation $\omega_k = Dk^2 + \Delta$ where $D = 2JSa^2$ for a simple cubic lattice and the spin-wave energy gap $\Delta = 0$.

[21] T. G. Perring, G. Aeppli, S. M. Hayden, S. A. Carter, J. P. Remeika, and S-W. Cheong, Phys. Rev. Lett. **77**, 711 (1996).

[22] M. C. Martin, G. Shirane, Y. Endoh, K. Hirota, Y. Moritomo, and Y. Tokura, Phys. Rev. B **53**, 14 285 (1996).

[23] J. W. Lynn, R. W. Erwin, J. A. Borchers, Q. Huang, and A. Santoro, Phys. Rev. Lett. **76**, 4046 (1996). The spin-wave stiffness was not measured at low temperatures by Lynn *et al.* but rather extrapolated to zero temperature from data at $T \geq 150$ K.

[24] S. E. Lofland, S. M. Bhagat, C. Kwon, S. D. Tyagi, Y. M. Mukovskii, S. G. Karabashev, and A. M. Balbashov, J. Appl. Phys. (to be published).

[25] A. Asamitsu, Y. Moritomo, Y. Tomioka, T. Arima, and Y. Tokura, Nature (London) **373**, 407 (1995).

[26] *CRC Handbook of Chemistry and Physics*, edited by R. C. Weast (CRC Press, Inc., Boca Raton, FL, 1990), p. E-82.

[27] J. Zaanen, G. A. Sawatzky, J. W. Allen, Phys. Rev. Lett. **55**, 418 (1985).